ISSN 1052-6188, Journal of Machinery Manufacture and Reliability, 2008, Vol. 37, No. 2, pp. 176–185. © Allerton Press, Inc., 2008.
Original Russian Text © V.A. Glazunov, S. Briot, V. Arakelyan, M.M. Gruntovich, Ngyuen Minh Thanh, 2008, published in Problemy Mashinostroeniya i Nadezhnosti Mashin, 2008, No. 2, pp. 90–100.

AUTOMATION AND CONTROL IN MACHINERY MANUFACTURE

Development of Manipulators with a Parallel-Cross Structure

V. A. Glazunov, S. Briot, V. Arakelyan, M. M. Gruntovich, and Ngyuen Minh Thanh

Moscow (Russia), Rennes (France), and Ho Chi Min City (Vietnam)

Received October 11, 2007

Abstract—Manipulators of a new class characterized by a parallel-cross structure are considered. Kinematic chains located according to the principles of a parallel structure are linked with cross chains that contain drives or impose constraints. Such a layout may facilitate a decrease in the dimensions of the foundation and the output link and an increase in stiffness. A classification of the proposed mechanisms is presented. The working volumes of the new manipulators and those of the most popular manipulators based on a parallel structure (the Gough–Stewart platform) are compared.

DOI: 10.3103/S1052618808020143

In recent years, many publications have been devoted to parallel-structure manipulators [1–6] owing to their unique capacity to bear large loads and ensure high accuracy. However, such mechanisms are characterized by inferior indicators with regard to the working volume and the capacity to ensure different orientations of the output link. This is due to the fact that the presence of many parallel kinematic chains results in their interference, i.e., in the appearance of contacts between links. Additionally, it is possible that driving kinematic chains located between the foundation and the output link ensure high stiffness along only one direction, with the stiffness characteristics along other axes being significantly lower.

Another factor that may limit the applicability of parallel-structure mechanisms may be the necessity of locating many elements related to the kinematic pair of driving chains on the foundation and the output link. This may result in an increase in the dimensions of the foundation and the output link and, consequently, of the mechanism as a whole.

In this study, an alternative to these manipulators is proposed in the form of mechanisms with a parallel-cross structure that are characterized by the location of cross kinematic chains, which contain drives or impose constraints, between several kinematic chains arranged according to parallel-structure concepts. This approach may enable some increase in the working volume since the kinematic chains are now less subject to interference. Additionally, stiffness may increase in the directions perpendicular to the location of parallel kinematic chains. The proposed engineering solutions involve some disadvantages; in particular, the design of the structures of the parallel kinematic chains to which elements of the cross chains are fixed becomes more complex. The proposed class of mechanisms may be relatively broad, as is indicated by the presented classification based on the number of degrees of freedom and the number of parallel and cross kinematic chains.

To compare the proposed manipulators with already existing ones, in this study, we compare the working volumes of the two most popular parallel-structure mechanisms (Gough and Stewart platforms) with the working volumes of two newly developed mechanisms. In one of these mechanisms, drives are located within the working space, and in the other, they are located outside the working space. Owing to this, the mechanism may be used in a corrosive environment, e.g., in vacuum.

The working volumes are compared under the following conditions. First, the constraints are considered that are imposed by the design of linear actuators, namely, the maximal and minimal rod extensions. Then the constraints related to the design of kinematic pairs (the maximal rotation angle) are imposed. Next, the conditions of interference between links are taken into account. Then the limitations related to the requirements set for mechanisms are applied, namely, the permissible pressure angle, the limiting minimal stiffness, and the minimal number of orientations of the output link that is determined at each studied point of the working volume. The orthogonal coordinates of the center of the output-link coordinate system are studied within a preset parallelepiped in the interior of which they are scanned with some step. The orientations of this link are considered in a similar way.

We now consider a description and classification of the proposed mechanisms belonging to the new class. Their main difference from parallel-structure mechanisms is that the kinematic chains located in parallel are interrelated with cross-located kinematic chains. We present their classification signatures.

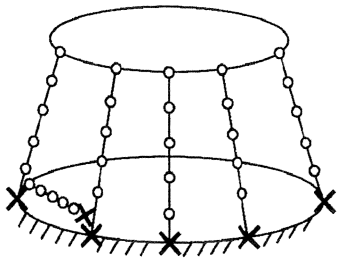

Fig. 1.

Similarly to the approach used for parallel-structure mechanisms [5, 6], the list of the classification signatures includes the number of degrees of freedom, the number of kinematic chains with a sequential location of links, and (this is characteristic of this class of mechanisms) the relation between the number of kinematic chains located in parallel and across. The number of degrees of freedom m may be determined from the known formula $m = 6n - 5p_5 - 4p_4 - 3p_3$, where n is the number of mobile links and p_5, p_4, and p_3 are the numbers of pairs belonging to a certain class.

However, to develop a classification, we use the fact that, in the absence of any constraints imposed by kinematic chains, the output link has six degrees of freedom. Each ith chain with a sequential location of links that contains no more than six pairs of the fifth class should impose D_i constraints and/or contain one or more drives. The number of constraints imposed by a chain is

$$D_i = 6 - p_5, \tag{1}$$

where p_5 is the number of kinematic pairs of the fifth class in this kinematic chain (pairs of other classes may be represented as a set of pairs of the fifth class).

We determine the number of degrees of freedom m using relation (1),

$$m = 6 - (D_1 + D_2 + \ldots + D_k), \tag{2}$$

where k is the number of kinematic chains.

We use formulas (1) and (2) to classify mechanisms belonging to the new class. Table 1 shows the variants that differ by the number of degrees of freedom and the number of kinematic chains. For each variant, the kinematic chains located in parallel are shown to the left and the chains located across are shown to the right. Each digit corresponds to the number of kinematic pairs of the fifth class in the corresponding kinematic chain. According to Table 1, there are 118 base schemes of mechanisms belonging to the considered class. A more detailed classification may be developed; for example, variants with six kinematic chains may be classified by the number of kinematic chains located in parallel and the number of cross chains (Table 2).

Afterward each of the base variants was represented in a graphical form. This presentation requires much space and is not shown here in full. We represent only one mechanism (Fig. 1) that has six kinematic chains of which five are located in parallel and one is located across. In Fig. 1, nondriving kinematic pairs are shown as circles and driving pairs are shown as crosses. This mechanism has six degrees of freedom. One more factor that affects operability should be noted. In designing such mechanisms, one should take into account that each closed loop should contain no less than seven fifth-class pairs; otherwise it will be a truss.

We consider in more detail the development of two mechanisms of the new class with six degrees of freedom and six kinematic chains of which three are located in parallel and three are located across (Fig. 2). Two variants of the drive location may be found. In the first case, all actuators are located in the working zone, i.e., on the same side of the foundation as the output link (Fig. 2a). In the second case, the actuators are located outside the working zone (Fig. 2b). Spherical kinematic pairs may be designed as a set of rotating pairs (Fig. 2c).

Each mechanism comprises a foundation (fixed link $A_1A_2A_3$) and a mobile platform (output link $B_1B_2B_3$). The output link is connected with the foundation by three spherical pairs each of which contains two spherical pairs with the centers located at points A_i and B_i and one driving translational pair whose axis is oriented along segment A_iB_i ($i = 1, \ldots, 3$). Additionally, these three kinematic chains are connected with each other by three more chains that comprise two spherical pairs with the centers at points C_i and D_j and one driving translational pair whose axis is oriented along segment C_iD_j ($j = i + 1$ for $i = 1, 2$ and $j = 1$ for $i = 3$). If spherical pairs B_i and D_i are represented as a Cardan joint (Fig. 2c), the number of mobile links is $n = 13$, the number of pairs of the corresponding classes $p_5 = p_4 = p_3 = 6$, and each mechanism has six degrees of freedom.

We denote displacements in translational pairs A_iB_i as ρ_i ($i = 1, \ldots, 3$) and in translational pairs C_iD_j as ρ_{i+3} ($j = i + 1$ for $i = 1$ and 2 and $j = 1$ for $i = 3$). We assume that triangles $A_1A_2A_3$ and $B_1B_2B_3$ are equilateral triangles. The center of the coordinate system of the output link is located at point P, which is the center of

Table 1

Number of kinematic chains	Number of degrees of freedom					
	6	5	4	3	2	1
6	66666–6 6666–66 666–666	56666–6 66666–5 5666–66 6666–65 566–666 666–665	55666–6 56666–5 5566–66 5666–65 6666–55 556–666 566–665 666–655	55566–6 55666–5 5556–66 5566–65 5666–55 555–666 556–665 566–655 666–555	55556–6 66555–5 5555–66 6655–55 6555–65 666–566 665–555 655–655	55555–6 55556–5 5555–56 5556–55 555–556 556–555
5	6666–6 666–66	5666–6 6666–5 566–66 666–65	4666–6 6666–4 5566–6 5666–5 466–66 666–64 556–66 566–65 666–55	5556–6 555–66 556–65 566–55	5555–6 555–56 655–55	5555–5 555–55
4	666–6	566–6 666–5	466–6 556–6 566–5 666–4	366–6 666–3 456–6 466–5 566–4	356–6 366–5 656–3 455–6 456–5 566–4 555–5	355–6 356–5 556–3 445–6 446–5 456–4 455–5 555–4
3	66–6	56–6 66–5	55–6 56–5	45–6 46–5 65–4 36–6 66–5 55–5	26–6 66–2 35–6 56–3 36–5 44–6 46–4 55–4 54–5	25–6 26–5 65–2 35–5 55–3 44–5 45–4

triangle $B_1B_2B_3$. The position of point P is set by the vector $[x, y, z]^T$. The center O of the base coordinate system coincides with the center of triangle $A_1A_2A_3$. The x_0 axis of the base coordinate system is oriented parallel to segment A_1A_2 and the y_0 axis is directed along segment OA_3.

The platform orientation is set by the angles α, β, and γ of rotation around axes z_0, x_1, and y_2, respectively. The indices show that the axes were modified after corresponding rotations.

Table 2

Number of kinematic chains		Number of degrees of freedom					
		6	5	4	3	2	1
6	5–1	66666–6	56666–6 66666–5	55666–6 56666–5	55566–6 55666–5	55556–6 66555–5	55555–6 55556–5
	4–2	6666–66	5666–66 6666–65	5566–66 5666–65 6666–55	5556–66 5566–65 5666–55	5555–66 6655–55 6555–65	5555–56 5556–55
	3–3	666–666	566–666 666–665	556–666 566–665 666–655	555–666 556–665 566–655 666–555	666–566 665–555 655–655	555–556 556–555

We now consider the problem of the positions of these mechanisms. The positions of points A_i, B_i, C_i, and D_i ($i = 1, 2, 3$) of a manipulator may be expressed in the following way:

$$\mathbf{OA}_i = \mathbf{curl}(\delta_i, z_0)\left[R_b\ 0\ 0\right]^T,$$

$$\mathbf{OB}_i = \begin{bmatrix} x \\ y \\ z \end{bmatrix} + \mathbf{curl}(\alpha, z_0)\mathbf{curl}(\beta, x_1)\mathbf{curl}(\gamma, y_2)\begin{bmatrix} R_{pl}\cos\delta_i \\ R_{pl}\sin\delta_i \\ 0 \end{bmatrix},$$

$$\mathbf{OC}_i = \mathbf{OA}_i + \frac{l_1}{\rho_i}\mathbf{A}_i\mathbf{B}_i, \quad \mathbf{OD}_i = \mathbf{OA}_i + \frac{l_2}{\rho_i}\mathbf{A}_i\mathbf{B}_i,$$

where the distances $R_b = OA_i$ and $R_{pl} = PB_i$; the angles $\delta_i = -5\pi/6, -\pi/6, \pi/2$ ($i = 1, 2, 3$) (since triangles $A_1A_2A_3$ and $B_1B_2B_3$ are equilateral); $l_1 = A_iC_i$, $l_2 = A_iD_i$; and Rot(ζ, w) is a matrix that describes the rotation by the angle ζ ($\zeta = \alpha$, β, and γ) around axis w of the variable coordinate system ($w = z_0$, x_1, and y_2).

Therefore, the expressions for the generalized coordinates have the following form:

$$\rho_i = \sqrt{(\mathbf{A}_i\mathbf{B}_i)^T(\mathbf{A}_i\mathbf{B}_i)} \quad (i = 1, 2, 3) \quad \text{and} \quad \rho_{i+3} = \sqrt{(\mathbf{C}_i\mathbf{D}_j)^T(\mathbf{C}_i\mathbf{D}_j)}$$
$$(j = i + 1 \quad \text{for} \quad i = 1, 2 \quad \text{and} \quad j = 1 \quad \text{for} \quad i = 3).$$

Thus, the problem of the positions is solved.

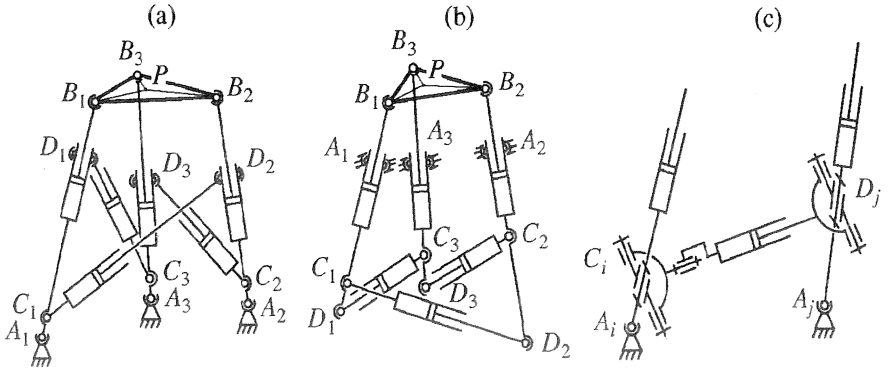

Fig. 2.

We now consider the equations of constraints that follow from the problem of the positions and partial derivatives of those equations. The equations of constraints have the following form:

$$f_i = 0 = \rho_i^2 - (\mathbf{A}_i\mathbf{B}_i)^T(\mathbf{A}_i\mathbf{B}_i) \quad (i = 1, 2, 3),$$

$$f_{i+3} = 0 = \rho_{i+3}^2 - (\mathbf{C}_i\mathbf{D}_j)^T(\mathbf{C}_i\mathbf{D}_j) \quad (j = i+1 \text{ for } i = 1, 2;\ j = 1 \text{ for } i = 3).$$

Differentiating these equations by time, we arrive at the following equations [7]:

$$\mathbf{A}\mathbf{v} + \mathbf{B}\dot{\mathbf{q}} = 0, \quad \mathbf{A} = \left[\frac{\partial f_i}{\partial X_i}\right], \quad \mathbf{B} = \left[\frac{\partial f_i}{\partial \rho_i}\right], \quad X_i = (x, y, z, \alpha, \beta, \gamma),$$

where **A** and **B** are two matrices, $\dot{\mathbf{q}} = [\dot\rho_1, \dot\rho_2, \dot\rho_3, \dot\rho_4, \dot\rho_5, \dot\rho_6]^T$ is the vector of generalized velocities, and $\mathbf{v} = [\dot x, \dot y, \dot z, \dot\alpha, \dot\beta, \dot\gamma]^T$ is the vector of the time derivatives of the absolute coordinates of the output link–platform.

Degenerate matrices yield different types of singular positions (singularities). If matrix **B** is degenerate, the kinematic screws that correspond to one kinematic chain are linearly dependent and the mechanism loses one degree of freedom [4–7]. This singularity corresponds to type 1. If matrix **A** is degenerate, the forcing screws transmitted to the output link from the side of kinematic chains are linearly dependent and the mechanism has an infinitely small uncontrolled mobility for one kinematic screw [4–7]. This singularity corresponds to type 2. There is a third type of singularity when both matrices (**A** and **B**) are degenerate.

Using transformation matrix **D**, vector **v** may be related with the kinematic screw **t** of the platform expressed in the fixed coordinate system [4]

$$\mathbf{t} = \mathbf{D}\mathbf{v}, \quad \text{where} \quad \mathbf{D} = \begin{bmatrix} \mathbf{I}_{3\times3} & \mathbf{0}_{3\times3} \\ \mathbf{0}_{3\times3} & \mathbf{L} \end{bmatrix}, \quad \mathbf{L} = \begin{bmatrix} 0 & \cos\alpha & -\sin\alpha\cos\beta \\ 0 & \sin\alpha & \cos\alpha\cos\beta \\ 1 & 0 & \sin\beta \end{bmatrix},$$

where $\mathbf{I}_{3\times3}$ and $\mathbf{0}_{3\times3}$ are the unit and zero 3×3 matrices, respectively.

Therefore, the Jacobi matrix **J** that relates the kinematic screw **t** of the platform with the generalized velocities $\dot{\mathbf{q}}$ has the following form:

$$\mathbf{J} = -\mathbf{D}\mathbf{A}^{-1}\mathbf{B}.$$

Matrix **A** has the following form:

$$\mathbf{A} = -2\begin{bmatrix} x_{B1}-x_{A1} & y_{B1}-y_{A1} & z_{B1}-z_{A1} & a_{14} & a_{15} & a_{16} \\ x_{B2}-x_{A2} & y_{B2}-y_{A2} & z_{B2}-z_{A2} & a_{24} & a_{25} & a_{26} \\ x_{B3}-x_{A3} & y_{B3}-y_{A3} & z_{B3}-z_{A3} & a_{34} & a_{35} & a_{36} \\ a_{41} & a_{42} & a_{43} & a_{44} & a_{45} & a_{46} \\ a_{51} & a_{52} & a_{53} & a_{54} & a_{55} & a_{56} \\ a_{61} & a_{62} & a_{63} & a_{64} & a_{65} & a_{66} \end{bmatrix},$$

where $a_{ik} = \dfrac{\partial x_{Bi}}{\partial\zeta}(x_{Bi}-x_{Ai}) + \dfrac{\partial y_{Bi}}{\partial\zeta}(y_{Bi}-y_{Ai}) + \dfrac{\partial z_{Bi}}{\partial\zeta}(z_{Bi}-z_{Ai})$ and $\zeta = (\alpha, \beta, \gamma)$ for $i = 1, 2, 3$ and $k = 4, 5, 6$. Other components of matrix **A** are described by more complex expressions and are not presented here.

Matrix **B** has the following form:

$$\mathbf{B} = \begin{bmatrix} 2\rho_1 & 0 & 0 & 0 & 0 & 0 \\ 0 & 2\rho_2 & 0 & 0 & 0 & 0 \\ 0 & 0 & 2\rho_3 & 0 & 0 & 0 \\ \partial f_4/\partial\rho_1 & \partial f_4/\partial\rho_2 & 0 & 2\rho_4 & 0 & 0 \\ 0 & \partial f_5/\partial\rho_2 & \partial f_5/\partial\rho_3 & 0 & 2\rho_5 & 0 \\ \partial f_6/\partial\rho_1 & 0 & \partial f_6/\partial\rho_3 & 0 & 0 & 2\rho_6 \end{bmatrix}.$$

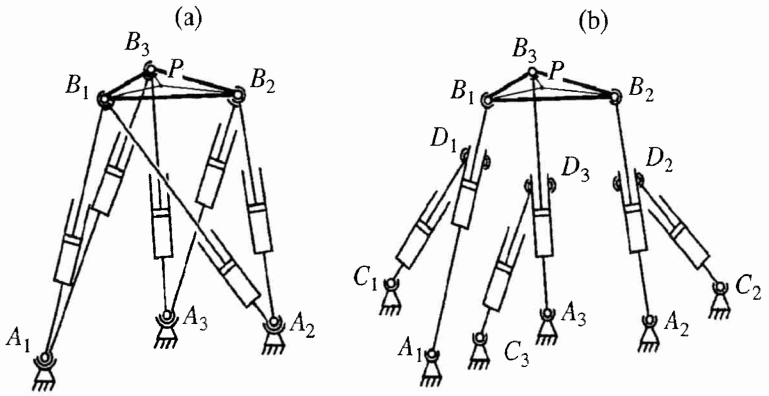

Fig. 3.

The elements of matrix **A** for $i = 1, 2, 3$ may be expressed as

$$\frac{\partial f_{i+3}}{\partial \rho_i} = -2\frac{l_1}{\rho_i^2}(x_{Bi} - x_{Ai})\left(x_{Aj}\left(1 - \frac{l_2}{\rho_j}\right) + \frac{l_2}{\rho_j}x_{Bj} - x_{Ai}\left(1 - \frac{l_1}{\rho_i}\right) - \frac{l_1}{\rho_i}x_{Bi}\right)$$

$$-2\frac{l_1}{\rho_i^2}(y_{Bi} - y_{Ai})\left(y_{Aj}\left(1 - \frac{l_2}{\rho_j}\right) + \frac{l_2}{\rho_j}y_{Bj} - y_{Ai}\left(1 - \frac{l_1}{\rho_i}\right) - \frac{l_1}{\rho_i}y_{Bi}\right)$$

$$-2\frac{l_1}{\rho_i^2}(z_{Bi} - z_{Ai})\left(z_{Aj}\left(1 - \frac{l_2}{\rho_j}\right) + \frac{l_2}{\rho_j}z_{Bj} - z_{Ai}\left(1 - \frac{l_1}{\rho_i}\right) - \frac{l_1}{\rho_i}z_{Bi}\right).$$

Other elements may be represented in a similar way.

We now compare the properties of the newly developed mechanisms with those of the parallel-structure mechanisms that are studied most widely [1, 2], i.e., the platforms proposed by Gough (Fig. 3a) and Stewart (Fig. 3b). Each of the mechanisms has six degrees of freedom and is driven by six linear drives (Fig. 3). The internal mobility that exists in the spherical pairs of each kinematic chain may be eliminated by using rotational pairs (Fig. 2c). The kinematic and force analysis of these mechanisms may be found in many studies and we will not consider it here in detail.

For the comparative analysis, we consider the same components of the existing and new mechanisms, namely, strokes of drive rods (ranges of variation of generalized coordinates) and the dimensions of the foundation and the output link. We determine which manipulator has larger dimensions of the working space taking into account the following factors: geometrical constraints (set limits for variations of generalized coordinates, limits for rotation angles in kinematic pairs, and possible interference between links); the value of the pressure angle in manipulators; the number of possible orientations of the mobile platform at points of the working space; and the bearing capacity of the manipulators, which is related with the stiffness of drives.

FANUC F200 is a popular robot that was developed on the basis of the Gough platform (which is sometimes referred to as the Stewart or Gough–Stewart platform). This manipulator is characterized by high bearing capacity and low compliance under the effect of a vertical force. We assume the following geometrical parameters: radii of the circles circumscribed around the mobile and immobile platforms $R_{pl} = 0.2$ m and $R_b = 0.3$ m, respectively, and drive rod strokes (ranges of variation of generalized coordinates) $(A_iB_i)_{\max} - (A_iB_i)_{\min} = 0.65$ m $(i = 1, \ldots, 6)$.

The structures of the considered mechanisms are different. Therefore, to make the comparison more justified, we select the closest values of the parameters of these mechanisms; namely, the parameters of the foundation and the output link should be the same for each manipulator and correspond to the set of parameters of a FANUC F200 robot, the drive rod strokes should be equal to 0.65 m, and all of the points that belong to the foundation should be located within triangle $A_1A_2A_3$.

Next we compare the working volume of the studied manipulators taking into account different limiting factors. The procedure used for determining the working space is as follows. The Cartesian space within which the output link moves is divided into n points and the possible orientation angles are divided into p orientations. The scanning step in the Cartesian space is 0.05 m and in the orientation space it is 10° for

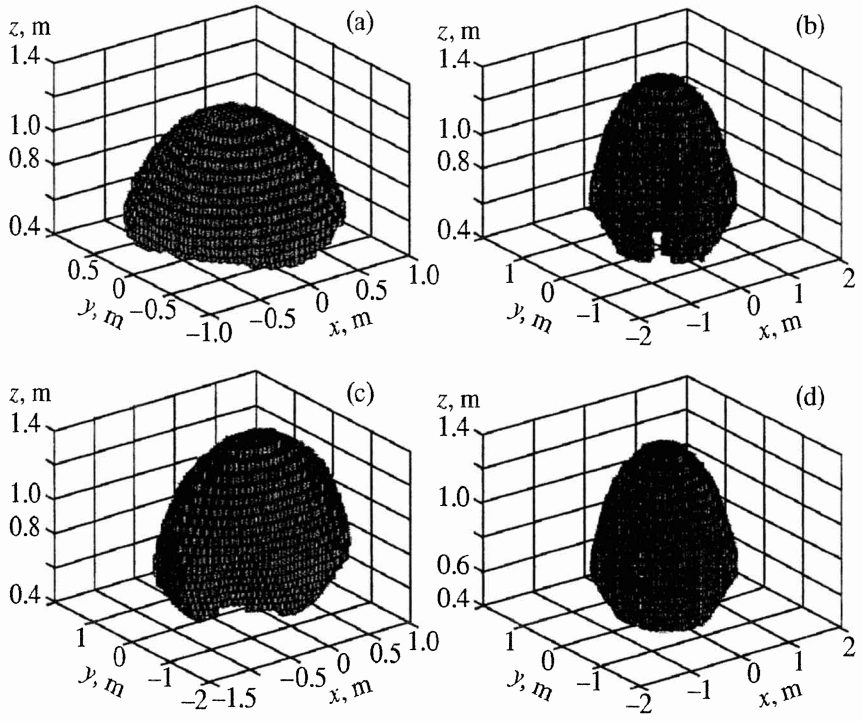

Fig. 4.

angles α, β, and γ varying from –60° to +60°. Point Q is considered to belong to the working space if at least one of the p orientations may be implemented at this point taking into account geometrical constraints. The corresponding characteristic may be associated with the maximal working volume [4].

The following geometrical constraints were imposed on the manipulator: the maximal drive rod stroke is 0.65 m; to prevent interference, the minimal distance between the links should be no less than 0.1 m; the minimal angle between two adjacent links connected with a hinge should be no less than 15° (for example, the angle between links A_iD_i and C_iD_i (Fig. 2c) should be no less than 15°); and the range of rotations in spherical pairs should range from –60° to +60°.

The geometrical parameters of the Gough platform are determined by the design of this manipulator. The geometrical parameters of other manipulators are assumed to be closest to the operational parameters of the FANUC F200 robot: for the Stewart platform, points C_1, C_2, and C_3 coincide with points A_2, A_3, and A_1, respectively, and $A_iD_i = 0.2$ m; for the first of the proposed manipulators (drives located within the working zone), $l_1 = 0.15$ m and $l_2 = 0.65$ m; and for the second manipulator (drives located outside the working zone), $l_1 = -0.3$ m and $l_2 = -0.75$ m.

As a result of the analysis of the working space (Fig. 4), we determined that the working volumes have the following values: (a) for the Gough platform, 0.719 m^3; (b) for the Stewart platform, 1.749 m^3; and for the manipulator with a parallel-cross structure, (c) 1.959 (variant 1) or (d) 2.168 m^3 (variant 2). This comparison has an approximate character since the considered mechanisms differ in their structure.

The next step in the study was to determine the parameters of the working space taking into account pressure angles. This characteristic is known to a larger extent for mechanisms with one degree of freedom [8, 9] and to a smaller extent for mechanisms with more than one degree of freedom [10]. The pressure angle is the angle between the direction of the force action and the direction in which the point to which this force is applied moves. For mechanisms with m degrees of freedom, it is necessary to consider m mechanisms with one degree of freedom fixing each time $m - 1$ drives. In singular position 2, the pressure angles are 90°.

It is known that, for a parallel-structure mechanism, the ith row in the inverse Jacobi matrix that relates the kinematic screw of a mobile platform with generalized velocities ($\dot{\mathbf{q}} = \mathbf{J}^{-1}\mathbf{t}$) represents the forcing screw $\mathbf{w}_i$ that corresponds to the ith drive. For a mechanism with six degrees of freedom, the inverse Jacobi matrix may be represented as

$$\mathbf{J}^{-1} = \begin{bmatrix} \mathbf{w}_1 \\ \vdots \\ \mathbf{w}_6 \end{bmatrix},$$

where all notations were explained above.

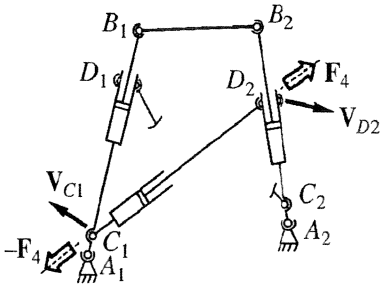

Fig. 5.

Without loss of generality, we consider the case where actuator 1 is not fixed and other actuators are fixed. The kinematic screw of the platform $\mathbf{t}_1$ is a screw that is reciprocal to the forcing screws $\mathbf{w}_2$, ..., $\mathbf{w}_6$ that act on the platform from the side of kinematic chains 2, ..., 6. This kinematic screw corresponds to five equations of reciprocity

$$0 = \upsilon_{1x}F_{ix} + \upsilon_{1y}F_{iy} + \upsilon_{1z}F_{iz} + \omega_{1x}M_{ix} + \omega_{1y}M_{iy} + \omega_{1z}M_{iz} \quad (i = 2, \ldots, 6),$$

where $\mathbf{V}_P = [\upsilon_{1x}, \upsilon_{1y}, \upsilon_{1z}]^T$ is the projection of the velocity of point P of the platform on the x, y, and z axes; $\mathbf{\Omega}_1[\omega_{1x}, \omega_{1y}, \omega_{1z}]^T$ is the projection of the angular velocity of the platform on the x, y and z axes; F_{ix}, F_{iy}, and F_{iz} are the projections of the vector of the force that acts from the side of the ith motor on the x, y, and z axes; and M_{ix}, M_{iy}, and M_{iz} are the projections of the torque that acts from the side of the ith motor on the x, y, and z axes.

Selecting coordinate υ_{1x} as the first coordinate, one can find other coordinates of kinematic screw $\mathbf{t}_1$:

$$\mathbf{t}_1 = \begin{bmatrix} 1 \\ -\mathbf{N}^{-1}\mathbf{F}_x \end{bmatrix}, \quad \text{where} \quad \mathbf{N} = \begin{bmatrix} F_{2y} & F_{2z} & M_{2x} & M_{2y} & M_{2z} \\ \vdots & \vdots & \vdots & \vdots & \vdots \\ F_{6y} & F_{6z} & M_{6x} & M_{6y} & M_{6z} \end{bmatrix}, \quad \mathbf{F}_x = [F_{2x}, F_{3x}, F_{4x}, F_{5x}, F_{6x}]^T.$$

For each considered manipulator, the forcing screw that acts from the side of drive 1 on point B_1 of the platform is a pure vector (zero-parameter screw) $\mathbf{F}_1$. Velocity $\mathbf{V}_{B1}$ of point B_1 may be expressed in the following way: $\mathbf{V}_{B1} = \mathbf{V}_P + \mathbf{B}_1\mathbf{P} \times \mathbf{\Omega}_1$, where all notations were defined above.

Thus, the pressure angle is $\alpha_1 = \cos^{-1}\left(\left|\dfrac{\mathbf{F}_1^T\mathbf{V}_{B1}}{|\mathbf{F}_1||\mathbf{V}_{B1}|}\right|\right)$.

It should be noted that the pressure angle expresses the power P that is transmitted from the side of drive 1 to the platform $P = \mathbf{F}_1^T\mathbf{V}_{B1} = |\mathbf{F}_1||\mathbf{V}_{B1}|\cos\alpha_1$. Therefore, if the angle α_1 is 90°, the power P is 0 and the manipulator cannot be activated by the corresponding drive. For a mechanism with six degrees of freedom, six pressure angles may be determined and afterward the most unfavorable of them may be selected. This method allows one to find all of the pressure angles for the Gough and Stewart platforms as well three of the six pressure angles for the proposed mechanisms. However, for actuators with numbers from four to six, the approach to determining pressure angles should be somewhat changed.

Without loss of generality, we consider link C_1D_2 (Fig. 5) for the new mechanisms. Using the considered mechanism, one can find the kinematic screw $\mathbf{t}_4$ of the platform where all of the drives except drive 4 are fixed. As a result, velocities may be determined $\mathbf{V}_{C1} = (l_1/\rho_1)\mathbf{V}_{B1}$ and $\mathbf{V}_{D2} = (l_2/\rho_2)\mathbf{V}_{B2}$.

The power transmitted from the drive side may be represented as $P = \mathbf{F}_4^T\mathbf{V}_{D2} - \mathbf{F}_4^T\mathbf{V}_{C1}$, where $\mathbf{F}_4$ is the direction of the vector of the force that acts from the actuator side on links A_1B_1 and A_2B_2. The power may be represented as $P = \mathbf{F}_4^T(\mathbf{V}_{D2} - \mathbf{V}_{C1}) = \mathbf{F}_4^T\mathbf{V}_{D2C1}$, where $\mathbf{V}_{D2C1}$ is the relative velocity of point D_2 with respect to point C_1. Therefore, the pressure angle is

$$\alpha_4 = \cos^{-1}\left(\left|\frac{\mathbf{F}_4^T\mathbf{V}_{D2C1}}{|\mathbf{F}_4||\mathbf{V}_{D2C1}|}\right|\right).$$

A similar expression may be derived for drives 5 and 6. It should be noted that the analysis of pressure angles is also an operation that allows the singular positions to be studied. A pressure angle is a static criterion of a singular position. This criterion restricts the working volume in a more stringent way than the kinematic criteria based on the linear dependence of screws or rows in a Jacobi matrix. The working volumes of the studied mechanisms may be analyzed on this basis. We assume that an angle of 82° is the maximal per-

missible pressure angle. If at some point of the working space there is at least one orientation where pressure angles are less than this value, this point belongs to the working space. The values of the working space are close to those obtained earlier, namely, 0.719 m^3 for the Gough platform, 1.727 m^3 for the Stewart platform, and 1.952 (variant 1) or 2.154 m^3 (variant 2) for a manipulator with a parallel-cross structure.

The next criterion for assessing the compared mechanisms is based on the number of possible orientations of the output link. In all of the cases considered above, $13^3 = 2197$ orientations were checked at each point of the working space and a point was considered to be suitable if at least one orientation was accessible. Now a new limitation is introduced and a point is considered to be suitable if no less than 200 orientations are accessible. In this case, we obtain values of the working space that are smaller than those obtained earlier, namely, 0.260 m^3 for the Gough platform, 0.953 m^3 for the Stewart platform, and 1.438 (variant 1) or 1.493 m^3 (variant 2) for a manipulator with a parallel-cross structure.

The next step in the comparison of the manipulators is related to the consideration of their loading capacity or stiffness. This characteristic depends on the stiffness of drives and configurations of mechanisms. We introduce the following notations: $\mathbf{w} = [F_x, F_y, F_z, M_x, M_y, M_z]^T$ is the forcing screw that acts on the output link (mobile platform); here, coordinates F_x, F_y, F_z, M_x, M_y, and M_z represent the force and the torque; $\boldsymbol{\tau} = [\tau_1, \tau_2, \tau_3, \tau_4, \tau_5, \tau_6]^T$ is the vector of the generalized forces that act in the drives; $\delta\mathbf{x} = [\delta x, \delta y, \delta z, \delta\alpha, \delta\beta, \delta\gamma]^T$ is the modified kinematic screw of an infinitesimally small motion of the mobile platform; δx, δy, and δz are coordinates of linear displacement; $\delta\alpha$, $\delta\beta$, and $\delta\gamma$ are coordinates of angular displacement; and $\delta\mathbf{q} = [\delta q_1, \delta q_2, \delta q_3, \delta q_4, \delta q_5, \delta q_6]^T$ is the vector of the elementary increments of the generalized coordinates.

The Jacobi matrix is known to yield a solution of the problem of force analysis. Indeed, according to the principle of virtual displacements, for an elementary increment of generalized coordinate δq_i, the expression for the elementary work yields

$$\delta q_i \tau_i = (\partial x/\partial q_i F_x + \ldots + \partial\gamma/\partial q_i M_z)\delta q_i, \quad \text{whence} \quad \tau_i = \partial x/\partial q_i F_x + \ldots + \partial\gamma/\partial q_i M_z.$$

Therefore, $\boldsymbol{\tau} = \mathbf{J}^T\mathbf{w}$, where $\mathbf{J}$ is the Jacobi matrix that relates the increments of the generalized and absolute coordinates $\delta\mathbf{x} = \mathbf{J}\delta\mathbf{q}$.

Considering stiffness in the drives, we obtain

$$\boldsymbol{\tau} = \mathbf{k}\delta\mathbf{q}, \quad \mathbf{k} = \begin{bmatrix} k_1 & 0 & \ldots & 0 \\ 0 & k_2 & \ddots & \vdots \\ \vdots & \ddots & \ddots & 0 \\ 0 & \ldots & 0 & k_6 \end{bmatrix},$$

where k_i is the elastic coefficient of the ith drive ($i = 1, \ldots, 6$).

This yields the displacement $\delta\mathbf{x}$ of the mobile platform as a result of the force action $\mathbf{w} = \mathbf{K}\delta\mathbf{x}$ and $\mathbf{K} = \mathbf{J}^{-T}\mathbf{k}\mathbf{J}^{-1}$, where all of the notations were introduced above.

In the analysis, we considered a load that acts in the horizontal plane. In this case the forcing screw is $\mathbf{w} = [F_x, F_y, 0, 0, 0, 0]^T$. The stiffness of the drives is assumed to be $k_i = 10000$ N/m ($i = 1, \ldots, 6$); this value is close to the stiffness in the FANUK F200 robot. First, this manipulator was considered and the maximal linear displacement was determined for the configurations specified in the cases above for the given loads in the horizontal plane. Therefore, the working volume for this mechanism remained unchanged. An assumption was made for all of the manipulators that a studied point belongs to the working space if no less than 200 orientations of the output link may be implemented and the linear displacement does not exceed the maximal displacement of the FANUK F200 robot. In this case, the dimensions of the working volume are less than those obtained earlier except for the robot mentioned above, namely, 0.260 m^3 for the Gough platform, 0 for the Stewart platform, and 0.814 m^3 (variant 1) or 0 (variant 2) for a manipulator with a parallel-cross structure.

In summary, manipulators of a new class that are characterized by a parallel-cross structure were presented. The mechanisms were classified and their working volumes were compared. Although such a comparison may not be considered as a strict one due to the difference between the structures of the considered mechanisms, we may conclude that mechanisms of the new class may be of significant practical interest.

REFERENCES

1. Gough, V.E., Contribution to Discussion to Papers on Research in Automobile Stability and Control and in Tire Performance by Cornell Staff, *Proc. Autom. Div. Inst. Mech. Eng.*, 1956, pp. 392–396.
2. Stewart, D.A., Platform with Six Degrees of Freedom, *Proc. Inst. Mech. Eng.*, 1965, vol. 180, part 1, no. 15, pp. 371–386.
3. Hunt, K., Structural Kinematics of In-Parallel-Actuated Robot Arms. *ASME. J. Mech. Transmissions, and Automation in Design*, 1983, vol. 105, pp. 705–712.
4. Merlet, J.-P., *Parallel Robots*, New York: Kluwer, 2000.
5. Glazunov, V.A., Koliskor, A.Sh., Krainev, A.F., and Model', B.I., Principles of Classification and Methods for Analysis of Spatial Mechanisms with a Parallel Structure, *Probl. Mashinostr. Nadezhnosti Mash.*, 1990, no. 1, pp. 41–49.
6. Glazunov, V.A., Koliskor, A.Sh., and Krainev, A.F., *Prostranstvennye mekhanizmy parallel'noi struktury* (Spatial Mechanism with a Parallel Structure), Moscow: Nauka, 1991.
7. Gosselin, C.M. and Angeles, J., Singularity Analysis of Closed-Loop Kinematic Chains, *IEEE Trans. Robotics and Automatics*, 1990, vol. 6(3), pp. 281–290.
8. Sutherland, G. and Roth, B., A Transmission Index for Spatial Mechanisms, *Trans. ASME. J. Eng. Industry*, 1973, vol. 95, pp. 589–597.
9. Lin, C.-C. and Chang, W.-T., The Force Transmissivity Index of Planar Linkage Mechanisms, *Mechanisms and Machine Theory*, 2002, vol. 37, pp. 1465–1485.
10. Arakelyan, V., Briot, S., and Glazunov, V., Improvement of Functional Performance of Spatial Parallel Manipulators Using Mechanisms of Variable Structure, *Proc. 12th World Congr. Mech. Machine Science*, France, 2007, vol. 5, pp. 122–128.